A simulation approach for predicting energy use during general milling operations

Stefano Borgia[a,1], Paolo Albertelli[b], Giacomo Bianchi[a]

[a] Institute for Industrial Technologies and Automation (ITIA), National Research Council of Italy (CNR), Via Corti 12, 20133, Milano, Italy

[b] Dept. of Mechanical Engineering, Politecnico di Milano, Via La Masa 1, 20156 Milano, Italy

Abstract

Manufacturing processes have a high impact on global energy consumption. Machine tools environmental impact is typically dominated by the energy absorbed during the use phase. Energy efficiency is progressively considered as an additional performance index in comparing alternative machines, process planning and machining strategies. For this purpose, this paper proposes a simulation approach that estimates the energy used by a machine tool in producing a generic workpiece by general milling operations. The developed tool simulates the execution of a standard ISO part program, basing on an explicit geometric and mechanistic representation of the cutting process, coupled with an energy model of the machine tool reproducing the power consumption of spindle, axes and auxiliary units. Energy models were identified by an experimental characterization procedure that can be easily adopted in industrial contexts. The simulator was validated comparing the estimated energy with measurements performed on different cutting tests, evaluating also its computational effort. Moreover, the simulator performances were compared to alternative energy evaluation methods proposed in the literature.

Keywords:

Machine tool, energy consumption, simulation, modeling

1 INTRODUCTION

Energy efficiency of machine tools has drawn wide attention in recent years since the high relevance of the sector in terms of yearly consumed energy (>10,000 PJ/y) [1]. The perpetual need to increase productivity and reliability of manufacturing processes has brought to high performance machines that are often characterized by a high energy demand [2]. As a consequence, energy saving is increasingly recognized as one of the important future goals in machine tool development and a concrete way to promote sustainability in manufacturing [3].

Recently European regulations have specifically addressed energy usage with the introduction of Directives dealing also with machine tools and production systems: Eco-design Directive for energy-using Products EuP 2005/32/EC [4] and Eco-design Directive for energy-related Products ErP 2009/125/EC [1]. According to the EuP Directive, CECIMO started a self-regulation initiative [5] to develop a new energy efficiency normative. In the meantime, the Commission mandated a preparatory study [6] to identify and recommend ways to improve the environmental performance of machine tools throughout their lifetime at their design phase. The International Organization for Standardization have been focusing on environmental evaluation of machine tool defining the norm ISO/TC 39/WG 12 14955 [7].

As demonstrated by [6] and [8], machine tools are products whose environmental impact is dominated by the use phase, in which they absorb great amounts of energy for transforming raw materials into finished products. In this scenario, approaches and methodologies that allow predicting the machine tool energy consumption required for processing a generic mechanical workpiece would be particularly useful. Recent scientific literature shows that many research efforts have been made in this direction. Indeed, energy consumption can be used as an additional performance index to compare alternative production systems (supporting also the design procedure), to assess different working conditions, to evaluate different process planning and machining strategies.

Some research contributions focused on machine tools energy assessment. First studies [9, 10] experimentally characterized the machine power requirements pointing out the role of the machine auxiliary equipment. The authors found that the total power demand can be generally differentiated into a fixed and a variable part that is proportional to the quantity of material being processed. The constant contribution is associated to the machine tool equipment typically required to support the process, while the variable one is related to the process physics.

Some existing works focused on machine tool energy modelling. For instance, Diaz et al. [8] and Kara and Li [11] developed empirical models that describe the relationship between the specific energy consumption (SEC, energy

[1] Corresponding and first author. Tel.: +39 (0)2 2369 9969; fax: +39 (0)2 2369 9915. E-mail address: stefano.borgia@itia.cnr.it (S. Borgia).

required by the machine for removing the unit of volume [J/cm3]) and the machining parameters. Draganescu et al. [12] performed a study of the influence of the main cutting parameters (feed rate, axial depth of cut, radial depth of cut, cutting speed and number of teeth) on both the machine tool efficiency and on specific energy consumption. A similar analysis was performed by Mori et al. [13] that presented a study on the effects of cutting parameters on total energy consumptions in face-milling operations. Other researches dealt with the energy optimization of metal cutting process conditions [14].

Scientific studies demonstrated that machine tool energy consumption can be used as an additional KPI. For instance, Newman et al. [15] reported some concrete examples: the experiments revealed that energy can be saved changing the machining strategies but without changing the total machining time. Pavanaskar et al. [16] similarly showed that the energy consumed for machining a specific feature can strongly depend on the adopted machining strategies. In this case, the optimized strategy guaranteed both the minimization of the consumed energy and the production time. Anderberg et al. [17] identified the process planning as one of the methodologies that can be exploited toward green machining.

In this scenario, a methodology able to estimate the energy required to process a workpiece, seems to be very useful. In order to tackle this issue, some research works proposed analytic and simulation approaches for estimating the machine tool power demand during its use. Avram and Xirouchakis [18] developed a simulation approach to estimate the power adsorbed by the spindle and feed axes during some selected simple 2.5 D milling operations. They showed that estimated power significantly differs from the average one estimated by traditional Life Cycle Analysis (LCA) techniques. Even if relevant improvements compared to traditional approaches were achieved, the adopted approach is not particularly suited for complex machining operations. Abele et al. [19] proposed an approach to simulate the energy consumption of machine tools for a specific production task by modeling the energy interactions of the machine tools components and implementing the models in a simulation environment. By connecting a hardware machine control system with the simulation model, NC-code information is utilized and machine tool specific characteristics of the simulation model behavior are achieved. As for the previous research, the approach can be satisfactorily used only for milling operations that involve simple tool-workpiece engagements. Moreover, the model needs many nominal parameters in order to be configured. Braun and Heisel [20] presented a model based approach for the prediction of the expected consumption of energy in turning operations. The whole simulation environment is based on a virtual CNC-Module that generates tool path data from given (simple DIN) G-Code sets. The tool trajectory is passed to a machine tool simplified model that considers mechanical and electrical components (e.g. drives and controller). A cutting model computes the tool-workpiece geometrical engagement for a given time step and outputs the resulting cutting forces that are fed back as external loads to the drive models for the power consumption computation. This work is very interesting but it is limited to turning operations.

This paper describes an approach to evaluate energy consumption of machine tools in operation, during the execution of a part program of milling operations on a generic workpiece. In this way is possible to investigate how different machining strategies influence the energy use, also on more complex geometries.

The developed simulator allows to compute the energy absorbed by each relevant machine element and points out the internal energy flows. Differently from the existing works (e.g. He et al. [21]), the proposed simulation approach is based on an explicit representation of the cutting process and its integration within the energy modeling of the machine tool. The simulator couples a detailed geometric simulation of the variable tool-workpiece engagement, where the tool is considered as a solid that removes material from the workpiece. An average cutting torque/force computation is performed through a mechanistic milling model, avoiding the complexity of computing the instantaneous forces generated by each single cutter.

The energy behavior of spindle and axis elements (equipping the totality of the machines) is investigated. In particular, an electrospindle based on a brushless motor with a defluxing controller is considered [22]. The focus on these machine components is motivated by the fact that servo-driven axis and spindle work, directly influenced by the cutting process, determines a non-negligible contribution to the machine tool total power consumption [13]. The other machine modules (i.e. auxiliaries, chillers, pumps, tool changer, etc.) and their energy consumption are modelled according to a modular approach [23], but they are not taken into account in the present paper.

According to [22], both the spindle system and the machine axis were modelled and characterized through the use of experimental characterization procedures that can be easily adopted in industrial contexts. It eases the model configuration on the base of the selected machine tool. The developed simulation approach was experimentally verified on different milling operations in terms of energy predicting capabilities and computational effort. Simulator performances were compared to the results achievable adopting other existing approaches [9].

The paper is organized as follows. The next section presents the architecture of the developed simulation approach for machine energy consumption estimation. The third section describes the adopted energy-oriented representation of the

cutting process and the proposed models for energy consumption estimation of spindle and axes subsystems. The fourth and fifth sections respectively present the selected reference application and the validation of the simulation approach. Finally the last section gives the conclusions and indicates some directions for further research.

2 APPROACH FOR ENERGY SIMULATION OF MACHINE TOOL

This paper proposes a modular modeling approach for energy evaluation of machine tools. Machine energy consumption is modelled by connecting the energy models of its elements (i.e. mechanical, electrical, hydraulic, or pneumatic devices), representing the energy fluxes between them, i.e. the thermal load of the spindle toward the chiller, the cooling action of the chiller on spindle and axes, etc. The cutting process is considered as entity that transmits a load: cutting torque and forces have to be overcome by spindle and axes motors, whose action has a downstream impact on the peripherals energy behavior. So, geometric and mechanistic representations of the cutting process are integrated within the energy simulation, allowing an explicit computation of the energy required by the machine modules.

The machine simulator architecture (see Fig. 1) is composed by the following modules: Numerical Control Emulator, Geometric Engine, Milling Process Model and Energy Evaluator.

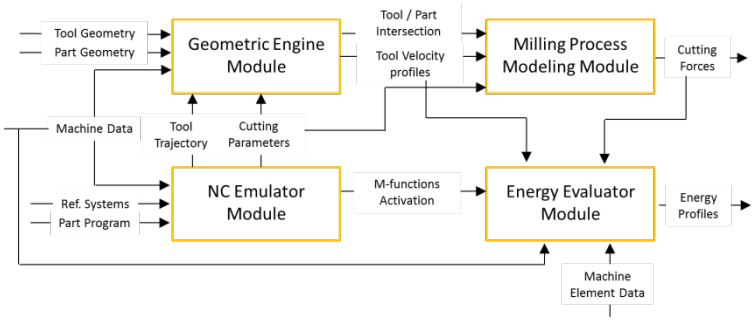

Fig. 1: Energy simulator of machine tool.

A brief description of each module is provided in the following.

Numerical Control Emulation Module. In this first release of the simulator, the NC emulation module is an executable demo-software, "SimuCN", developed by NUM [24]. This software parses the ISO part program and, taking into account the kinematic properties of the machine axes (maximum speed and accelerations), applies a look-ahead strategy and computes the instantaneous reference position and speed of each axis along a generic tool path. Data are saved at the sampling time of the position controller (typically few milliseconds).

Geometric Engine Module. Having defined tools and part data, the geometric engine computes tool-workpiece engagement and material removal rate. This module is based on commercial CSG (Computational Solid Geometry) libraries: together with the developed C++ functions, they provide methods and structures for solid intersection, allowing the computation of MRR, depth of cut and engagements arcs, used by the developed cutting process models.

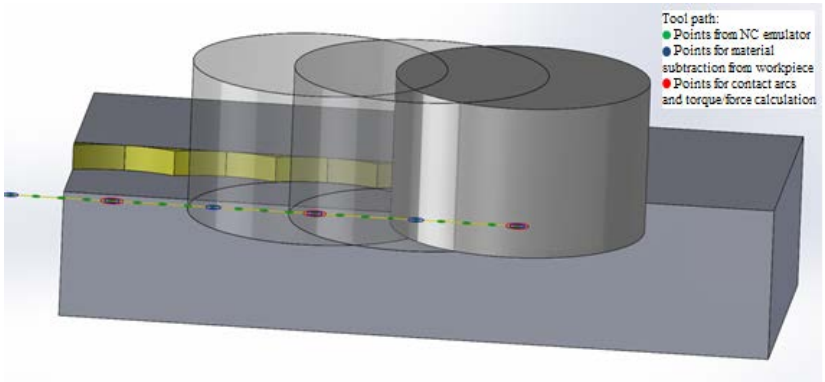

Fig. 2: example of the conceived approach for the geometric simulation of a milling operation

Fig. 2 exemplifies the conceived approach of geometric simulation, based on a "small-step subtraction" algorithm. Since geometrical evaluation is the most time consuming phase of the whole simulation, specific solutions have been implemented to optimize the compromise between accuracy and computational effort. Adequate accuracy must be

obtained for all output data along the path, passed to the subsequent cutting process and machine energy models: actual time, axis velocities and accelerations, removed material and cutting forces.

In the Geometrical Engine the tool path is represented through a 3d spline curve that interpolates the axis reference position data (the green points in Fig. 2) imported from the NC emulator. The tool, represented by a cylinder, is moved on a series of subsequent points (the blue ones in Fig. 2) obtained by a discretization of the tool path, usually defined proportionally to the tool radius. For each simulation step, the tool-workpiece intersection volume is removed from the workpiece and the corresponding values of time, feed rate and spindle speed are obtained by linear interpolation of the NC data. Longer is the step between two consecutive points, less accurate is the calculation of the material removal. Material removal rate (MRR) is computed dividing the removed volume by the time interval required by the tool to cover the step distance. Only on a subset of these points (the red ones in Fig. 2), a second batch of geometrical computation is executed to calculate the geometrical data required by the cutting process model. Tool geometry is discretized in a set of sections along the Z axis, called slices, corresponding to a portion of depth of cut (Fig. 3-a). For each slice, tool-workpiece engagement arcs are computed (Fig. 3-b). Force computation is time consuming, so it would be, in theory, preferable to repeat the calculation only when forces and torque change. This strategy has been implemented by an heuristic logic that recognizes MRR variation along the tool path. As cutting forces, in particular cases, can change even with a constant MRR, their calculation is anyhow forced every N steps (e.g. 5 points).

The user has to define the following simulator parameters: resolution of the geometric environment, step distance for curve discretization and number of slices in which the tool has to be sectioned. The values of these data have a relevant impact on simulation duration and accuracy, investigated in chapter 5.4.

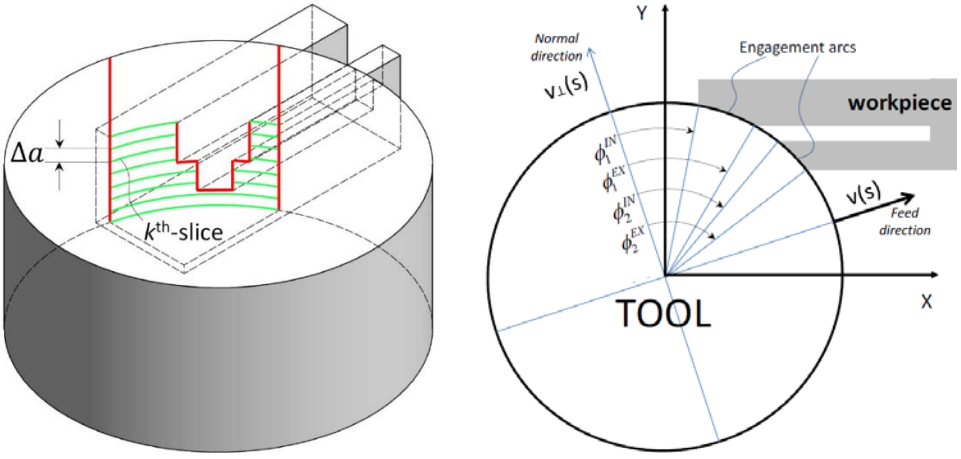

(a) (b)

Fig. 3: Slicing of the workpiece-tool intersection and engagement arcs definition.

Cutting Process Modeling Module. The cutting effort is computed as "average instantaneous" cutting torque and forces, without considering the high frequency periodicity due to the actual defined cutting tools, taking into account cutting parameters, workpiece material and tool geometry. Torque is calculated from the computed material removal rate, while forces are estimated for each tool slice, from the engagement arcs provided by the geometric engine. For details, ref. section 3.3.

Energy Evaluator Module. The energy evaluator (implemented in Matlab Simulink/SimScape) receives information extracted from the other modules (i.e. axis position, speed and acceleration; cutting forces and torque) and performs the energy simulation of the whole machine, including the peripherals units,. The most energy significant elements of a machine tool – e.g. drives, spindle and axes, cooling systems, hydraulic units, etc. – are represented through a library of developed mathematical models [23]. Machine configuration has to be defined before running simulations. Similarly, models parameters have to be set or identified for the specific machining center under exam.

The execution of all simulator modules is driven and managed by a main program implemented in Matlab environment.

Since the aim of this work is to evaluate the accuracy of the cutting-process model, the analysis is focused on spindle and axis drives, described in the following chapter.

3 ELECTRO-MECHANICS MODELING OF MACHINE TOOL

3.1 Spindle energy modeling

The electro-spindle is the component most directly associated to the process power demand, delivering the required speed and torque. Modern spindles often use AC permanent magnet synchronous motors (PMSM, brushless): they are characterized by a high torque to mass ratio but, to reach high speeds, require a control strategy, called “defluxing”, able to reduce the excitation field produced by permanent magnets. The energy model is constructed considering an electrical power consumption P_{spn} [W] calculated as the sum of the mechanical output power $P_{spn.M}$ and the power $P_{spn.R}$ dissipated through the motor winding resistances (Eq. 1):

$$P_{spn} = P_{spn.M} + P_{spn.R} = T_{spn.m} \cdot \omega_r + R_s \cdot i^2 \qquad \textbf{Eq. 1}$$

where: $T_{spn.m}$ is the resistant torque [Nm] on the spindle motor, ω_r is the rotor velocity [rad/s], R_s is the phase resistance [Ω] and i is the current [A].

Permanent magnets brushless motors have stator windings which generate a rotating current phasor $\mathbf{I}$. Considering the usual d-q (direct-quadrature) rotating reference system, where the d-axis is oriented as the permanent magnetic flux ϕ_r [Wb], the current phasor can be split into two parts: the q-axis component i_q [A_{rms}], that generates a magnetic flux orthogonal to ϕ_r [Wb] and produce torque, and the d-axis component i_d [A_{rms}], that is used to weaken the excitation flux when necessary. Similarly, voltage phasor components v_d and v_q along the two axes can be derived, defining the instantaneous value numerical model of Eq. 2, where L_q is the q-axis inductance [H], L_d is the d-axis inductance [H] and p is the number of pole couples.

$$\mathbf{V} = \begin{bmatrix} v_d \\ v_q \end{bmatrix} = \begin{bmatrix} R_s \cdot i_d + L_d \cdot \dfrac{\partial}{\partial t} i_d - p \cdot \omega_r \cdot L_q \cdot i_q \\ R_s \cdot i_q + L_q \cdot \dfrac{\partial}{\partial t} i_q + p \cdot \omega_r \cdot L_d \cdot i_d + p \cdot \omega_r \cdot \phi_r \end{bmatrix} \qquad \textbf{Eq. 2}$$

The expression of the motor electromagnetic torque M_e in d-q reference system is shows in Eq. 3. The first term of the torque is due to the interaction between stator current and rotor flux; the second term is the reluctance torque, due to the presence of magnetic anisotropy and parasite currents. Assuming the common hypothesis of motor magnetic isotropy, the reluctance torque is zero ($L_q = L_d$) and so torque only depends on the quadrature current i_q [A_{rms}], even in field weakening conditions.

$$M_e = \frac{3}{2} \cdot p \cdot i_q \cdot \left[\phi_r + \left(L_q - L_d \right) \cdot i_d \right] = \frac{3}{2} \cdot p \cdot \phi_r \cdot i_q \qquad \textbf{Eq. 3}$$

Motor operation, for required values of speed and torque, depends on the adopted control strategy that must comply with voltage, current and flux limitations of the motor-drive system. Common field weakening control strategies maximize the torque / current ratio, imposing, when required, a negative stator direct current. According to operative conditions and limits, the quadrature current (rms value) and direct current can be computed as in Eq. 4 and Eq. 5:

$$i_q = \frac{2}{3} \cdot \frac{M_e}{p \cdot \phi_r} = \frac{T_{spn}}{k_t} \qquad \textbf{Eq. 4}$$

$$i_d = \begin{cases} 0 & \text{if } \left| i_q \right| \le \left| i_{q.0.\max}\left(\omega_r\right) \right| \\ -\dfrac{\phi_r}{L_d} + \sqrt{\left(\dfrac{V_L}{\omega_r \cdot p \cdot L_d} \right)^2 - {i_q}^2} & \text{if } \left| i_q \right| \ge \left| i_{q.0.\max}\left(\omega_r\right) \right| \end{cases} \qquad \textbf{Eq. 5}$$

where k_t is the spindle motor torque constant [Nm/A_{rms}], V_L is the bus voltage limit [V], $i_{q.0.\max}\left(\omega_r\right)$ is the maximum quadrature current that can be provided at given motor velocity without imposing field weakening. The spindle

mechanical torque T_{spn} provided by the motor is used not only for cutting (T_{cut}), but also for overcoming friction and for accelerating the spindle.

$$k_t \cdot i_q = T_{spn} = \mu_s \cdot sign(\omega_r) + \mu_v \cdot \omega_r + J \cdot \dot{\omega}_r + T_{cut} \qquad \textbf{Eq. 6}$$

In **Eq. 6**, $\dot{\omega}_r$ is the spindle acceleration [rad/s^2], μ_s is the static friction coefficient [Nm], μ_v is the viscous friction coefficient [Nm·s/rad], J is the moment of inertia [kg·m^2], T_{cut} is cutting torque [N].

3.2 Axes energy modeling

A simplified numerical modeling able to evaluate the electrical power necessary to move machine tool axes was proposed [23]. Axis power consumption P_{axis} is calculated as the sum of the mechanical output power $P_{axis.M}$ and the power dissipated through the motor resistances $P_{axis.R}$, as reported in Eq. 7. Assuming that the velocities imposed to machine tool axis do not require motor field weakening, the direct current can be considered null and the power depends only on the quadrature current. The power dissipated by the motor is represented, for the speed range of interest, by the term linked to the "copper" or Joule losses in the motor windings and by the frictions.

$$P_{axis} = P_{axis.M} + P_{axis.R} = k_t \cdot i_{q.rms} \cdot \omega + R_s \cdot {i_q}^2 \qquad \textbf{Eq. 7}$$

where $i_{q.rms}$ is the axis motor quadrature current (rms value) [A_{rms}], i_q is the axis motor quadrature current [A], ω is the axis motor velocity [rad/s], k_t is the axis motor torque constant [Nm/A_{rms}], R_s is axis motor stator resistance [Ω].

The mechanical power takes into account inertial, and frictional effects together with the contribution due to cutting forces F_c. For machine axes equipped with rotary motors, motor load can be expressed through Eq. 8. If linear motors are considered, rotation physical quantities have to be substituted by the corresponding linear ones.

$$k_t \cdot i_{q.rms} = T_{axis} = \mu_s \cdot sign(\omega) + \mu_v \cdot \omega + J \cdot \dot{\omega} + \frac{F_c}{\tau} \qquad \textbf{Eq. 8}$$

Where $\dot{\omega}$ is the axis motor acceleration [rad/s^2], μ_s is the static friction coefficient [Nm], μ_v is the viscous friction coefficient [Nm·s/rad], J is the inertia [kg·m^2], F_c is cutting force opposing axis motor [N], τ is the axis transmission ratio [rad/m], T_{axis} is the torque to be provided by the axis motor.

3.3 Cutting process modeling

A great amount of existing scientific works deals with cutting force modeling [25], but they are not usually tailored for energy analyses. Many authors describe the cutting process by means of a volumetric specific cutting energy associated to the removed material [8] [9], avoiding to consider the feed axes power adsorption.

Aiming at evaluating the influence of both axis and spindle drive load on the machine efficiency, in this work the energy for removing material in milling is computed integrating over time the motors power adsorption, considering both spindle and feed axes. Since the feed axes load depends also on the tool path and on the tool-workpiece engagement, the following properties for the cutting process modeling have to be fostered:

- High generality for handling any kind of tools and tool path with a limited set of force model parameters.
- Low computational time, allowing the analysis of complex machining cycles.

The developed modeling approach is obtained extending the formulation presented in [26], where the tool-workpiece engagement condition is described in terms of arcs of contact. In the most general case, the arcs of contact may be more than one for each tool section and may vary along the tool axis (see Fig. 3). The list of the contact arcs for each tool slice is computed by a dedicated code of the geometric engine module.

Even if all the harmonics of the cutting forces can contribute to motor power dissipation (due to the quadratic copper losses, Eq. 1, Eq. 3, Eq. 7 and Eq. 8), the developed formulation considers only the average cutting force value. The approximation error due to this assumption will be analyzed and verified in section 5.2.

Let's consider a planar milling operation, where the milling plane, defined w.r.t. to a global reference frame, is assumed to be XY; let f_v be the feed velocity [mm/min], oriented by a versor **v** w.r.t. the global reference frame (see Fig. 3). Considering the generic tool slice (k-th), the average cutting force pertaining to each arc (i-th) of contact in the local reference frame (feed (f), normal (n) and axial (a) components) is given by the following expression (Eq. 9). $\bar{F}_{f_{ik}}^{local}$, $\bar{F}_{n_{ik}}^{local}$ and $\bar{F}_{a_{ik}}^{local}$ are the cutting force components [N] along feed, normal and axial directions. Δa is the axial discretization step of the tool. k_{tc}, k_{rc}, k_{ac} are the tangential, axial and radial cutting pressures [N/mm^2], k_{te}, k_{re}, k_{ae} are the tangential, axial and radial edge coefficients [N/mm], $\varphi_{ex_{ik}}$, $\varphi_{st_{ik}}$ are the exit and starting angles [rad] defining the *i*-th engagement arc of the k-th slice (see Fig. 3 for definition), Ω is the spindle speed [rpm] and N is the number of tool teeth.

$$\begin{cases} \bar{F}_{f_{ik}}^{local} = \sum_{i,k} \operatorname{sgn}(\Omega) \cdot \Delta a \cdot \left\{ \begin{array}{l} \frac{f_v}{8\pi\Omega}\left[K_{tc} \cdot \cos 2\varphi - \operatorname{sgn}(\Omega) \cdot K_{rc}(2\varphi - \sin 2\varphi)\right] + \\ + \frac{N}{2\pi}\left[-K_{te} \cdot \sin\varphi + \operatorname{sgn}(\Omega) \cdot K_{re} \cos\varphi\right] \end{array} \right\}_{\varphi_{st_{ik}}}^{\varphi_{ex_{ik}}} \\ \bar{F}_{n_{ik}}^{local} = \sum_{i,k} \operatorname{sgn}(\Omega) \cdot \Delta a \cdot \left\{ \begin{array}{l} \frac{f_v}{8\pi\Omega}\left[K_{tc} \cdot (2\varphi - \sin 2\varphi) + \operatorname{sgn}(\Omega) \cdot K_{rc} \cdot \cos 2\varphi\right] + \\ - \frac{N}{2\pi}\left[K_{te} \cdot \cos\varphi + \operatorname{sgn}(\Omega) \cdot K_{re} \sin\varphi\right] \end{array} \right\}_{\varphi_{st_{ik}}}^{\varphi_{ex_{ik}}} \\ \bar{F}_{a_{ik}}^{local} = \sum_{i,k} \operatorname{sgn}(\Omega) \cdot \Delta a \cdot \left[\frac{f_v}{2\pi\Omega}\left(-K_{ac} \cos\varphi\right) + \frac{N}{2\pi} K_{ae}\varphi \right]_{\varphi_{st_{ik}}}^{\varphi_{ex_{ik}}} \end{cases} \quad \textbf{Eq. 9}$$

The overall average cutting force components acting on the tool are given by the sum of the forces associated to each arc (Eq. 10), on all tool slices. Eq. 11 projects force components along the global reference frame:

$$\vec{\bar{\mathbf{F}}}^{local} = \left\{ \sum_{i,k} \bar{F}_{f_{ik}}^{local} \quad \sum_{i,k} \bar{F}_{n_{ik}}^{local} \quad \sum_{i,k} \bar{F}_{a_{ik}}^{local} \right\} \quad \textbf{Eq. 10} \qquad \vec{\bar{\mathbf{F}}}^{global} = \begin{bmatrix} v_x & -v_y & 0 \\ v_y & v_x & 0 \\ 0 & 0 & 1 \end{bmatrix} \cdot \vec{\bar{\mathbf{F}}}^{local} \quad \textbf{Eq. 11}$$

Dealing with helical end mills [26], cutting coefficients k_{tc}, k_{rc}, k_{ac} can be expressed as function of the helix angle α and the cutting coefficients related to normal and feed component of orthogonal cutting experiments (k_n for the component aligned with cutting velocity, k_f for the component aligned with feed velocity):

$$\begin{array}{ll} k_{tc} = k_n & k_{te} = k_{ne} \\ k_{rc} = \dfrac{k_f}{\cos\alpha} & k_{re} = \dfrac{k_{fe}}{\cos\alpha} \\ k_{ac} = k_n \tan\alpha & k_{ae} = k_{ne} \tan\alpha \end{array} \quad \textbf{Eq. 12}$$

An alternative model [26] consists in substituting the edge force components with an exponential correction of the cutting components with respect to the average chip thickness, namely:

$$k_{n_{ik}} = k_{n1} \cdot h_{m_{ik}}^{-M}$$
$$k_{f_{ik}} = k_{f1} \cdot h_{m_{ik}}^{-M} \qquad \textbf{Eq. 13}$$

where: k_{n1} and k_{f1} are the nominal cutting coefficients when a chip thickness of 1 mm is considered and $h_{m_{ik}}$ is the average chip thickness associated to the i-th engagement arc of the *k*-th slice, M is a correcting factor depending on the considered material.

The average chip thickness depends on feed rate as follows:

$$h_{m_{ik}} = \frac{f_v}{|\Omega|} \cdot \frac{1}{N} \cdot \frac{\cos\left(\varphi_{ex_{ik}}\right) - \cos\left(\varphi_{st_{ik}}\right)}{\varphi_{ex_{ik}} - \varphi_{st_{ik}}} \qquad \textbf{Eq. 14}$$

Both exponential correction and edge components aim at capturing the same evidence, namely, the fact that cutting force does not decrease proportionally when chip thickness tend to zero.

Cutting process torque on the spindle is computed through **Eq. 15**, including both T_c due to material removal and T_e related to the effect of the edge forces on the tool.

$$T_{cut} = T_c + T_e = \frac{MRR \cdot K_{tc}}{\Omega} + \frac{D}{2} \cdot \sum_{i,k} \operatorname{sgn}(\Omega) \cdot \Delta a \cdot \frac{N}{2\pi} \cdot K_{te} \left\{\varphi\right\}_{\varphi_{st_{ik}}}^{\varphi_{ex_{ik}}} \qquad \textbf{Eq. 15}$$

where: MRR is the instantaneous material removal rate (output of CSG engine) [mm^3/s] and Ω is the spindle speed (with sign), that corresponds to the motor speed in absence of the transmission ratio.

4 APPLICATION

The proposed simulation approach was tested on real milling operations. The cutting tests were performed by a Mandelli M5 CNC machining center (Fig. 4). The X, Y and Z axes are driven by synchronous rotary motors. The electro-spindle mounts hydrostatic oil bearings for high precision machining and is equipped by a permanent magnetic synchronous motor (110 [Nm] S1, 65 [kW]). A model parameter identification was performed considering the data acquired in a preliminary experimental session. The identification procedure was applied to machine tool components characterized by the highest energy consumption. For the experimentation, the Japanese standard [27] on power consumption test methods for numerically controlled machining centers was taken as references. The consumption of CN, drives, refrigerators (compressors and pumps), auxiliary devices, axis and spindle motorizations were evaluated through power measurements. It has to be noted that the analyzed machine tool is a prototype designed for experimental use and testing in laboratory. The presence of hydrostatics determines very high consumptions of auxiliary systems, such as the spindle pressure unit and chiller unit, that are not so significant of the energy behavior of typical machine tool. In any case the focus of the present paper regards the electro-mechanic subsystems, so the considered machining center represents a good application industrial case.

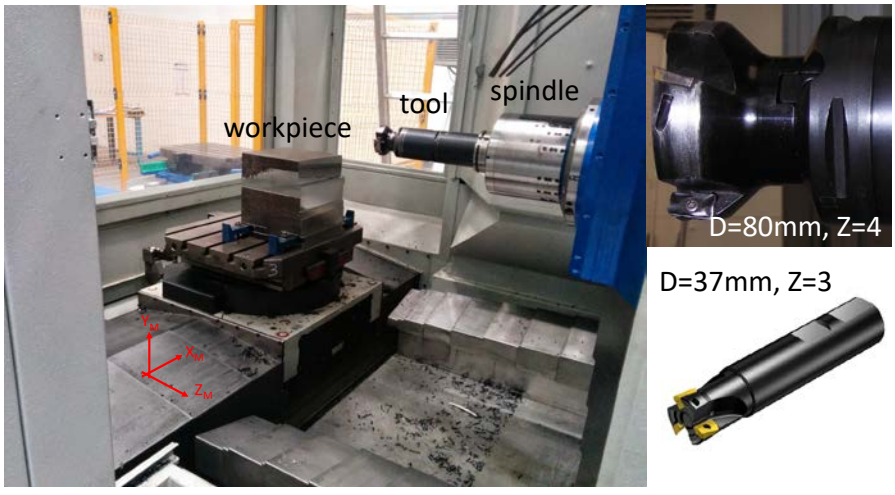

Fig. 4: Mandelli M5 machining center

Different measurement test campaigns were executed on the selected machining center. A first test session in load operation mode (no cutting) was exploited to machine energy modeling identification, allowing the estimation of the unknown parameters. Different cutting tests and a machining feature production were conducted to prove the energy prediction capacity of the proposed energy simulation approach - especially in comparison to other existing simplified models - and to validate the adoption of the defined energy-oriented cutting process modeling. Electrical and kinematic measurements have been acquired at spindle and axes motors and drives using external self-built power sensors, SinuCom NC (Siemens) software and a real time acquisition system.

5 VALIDATION

5.1 Spindle and axes energy models experimental identification and verification

Spindle and axes motor numerical models (Eq. 6 and Eq. 8) have been experimentally characterized by measuring quadrature current, velocity and power (with a sample frequency of 200 [kHz] for phase currents and voltages) during the execution of specific tests in "load operation mode" [27] without material removal (no cutting forces and torque):

- the spindle is rotated at different velocities (2500 [rpm], 3000 [rpm], 3500 [rpm], 4000 [rpm]);
- each axis is commanded with a part program which involves different axes movements.

During the characterization test, the motor load is only due to friction and inertia. A least square method is used to estimate the unknown parameters μ_s, μ_v and J of spindle and axes models (Eq. 6 and Eq. 8), representing the global friction and inertia. In Fig. 5 and Fig. 6, the matching between measured quadrature current (respectively for spindle and X-axis, taken as examples) and the estimated one is presented. Motor torque constant values were taken by motor catalogues and the phase resistances were measured by the means of a commercial multi-tester. Table 1 presents the values of the obtained model parameters.

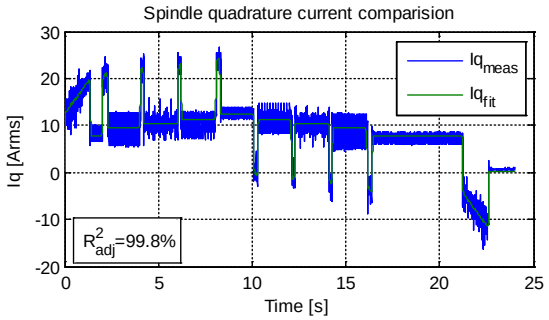

Fig. 5: Spindle model identification, fitted-measured quadrature current comparison

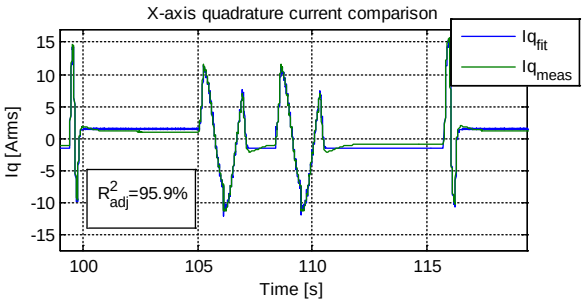

Fig. 6: X-axis model identification, fitted-measured quadrature current comparison

Table 1: Spindle and axis numerical model parameters

Parameter	Spindle	X-axis	Y-axis	Z-axis
Static friction μ_s [Nm]	0.144	2.753	2.188	2.499
Viscous friction μ_v [Nm·s/rad]	0.018	0.014	0.018	0.015
Inertia J [kg·m^2]	0.041	0.019	0.019	0.027
Torque constant k_t [Nm/A$_{rms}$]	0.638	1.81	1.81	1.81
Phase resistance R_s [Ω]	0.017	0.23	0.23	0.23

The adopted modelling approach (Eq. 1 and Eq. 7) was firstly verified computing the power consumption profile and the energy absorbed during the characterization tests. Measured power and the power estimated feeding the developed model with the kinematic quantities measured during the tests show a good match both for spindle and axes, as numerically reported in Table 2.

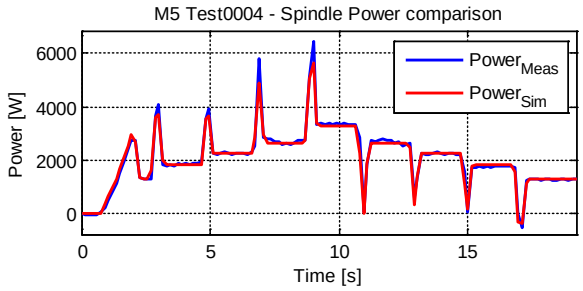

Fig. 7: Spindle model identification, estimated-measured electrical power comparison

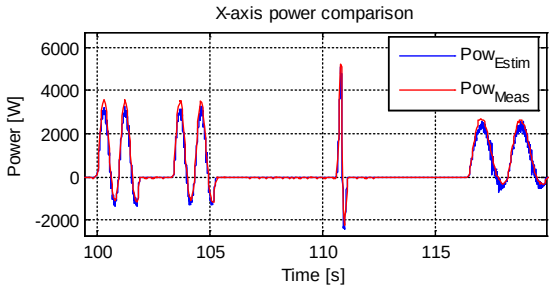

Fig. 8: X-axis model identification, estimated-measured electrical power comparison

Table 2: Model characterization tests, spindle and axes motor energy consumption comparison

Quantity	Spindle	X-axis	Y-axis	Z-axis
Estimated energy [kJ]	15.64	26.10	23.15	23.30
Measured energy [kJ]	16.24	27.10	24.07	24.91
Energy error [%]	-3.66%	-3.70%	-3.86	-6.48%

5.2 Validation of the energy simulation approach

The proposed simulation approach was validated on the following applications, with an increasing level of complexity and realism. Cutting experiments were executed in order to estimate the cutting and edge coefficients of the mechanistic modeling proposed for the cutting process (Eq. 9 and Eq. 15): k_{tc} 1660 [Nm/mm^2], k_{te} 91 [Nm/mm], k_{rc} 420 [Nm/mm^2], k_{re} 112 [Nm/mm]. During simulation, the geometric engine module parameters were set in a conservative way, in order to evaluate the performance in the best accuracy conditions: geometric resolution (tolerance) 10^{-4} [mm], distance step 1% of tool radius, number of slices 2. The effect of different simulator setup is explored in chapter 5.4.

Two milling tests with variable tool-workpiece engagement executed on a C45 steel stock with an end mill (ϕ 80 [mm], 4 inserts), see Fig. 9 and Fig. 10. The first cutting test regards the rectilinear milling operation (feed rate 900 [mm/min], spindle speed 920 [rpm], axial depth of cut 3 [mm]) of the upper surface of a workpiece on which an oblique slot was previously obtained with a preparatory operation, Fig. 9. The second cutting test consists of a rectilinear milling operation (feed rate 900 [mm/min], spindle speed 920 [rpm], axial depth of cut 3 [mm]) of the upper surface of a workpiece on which a previously machining process has been performed with a circular interpolated motion, Fig. 10.

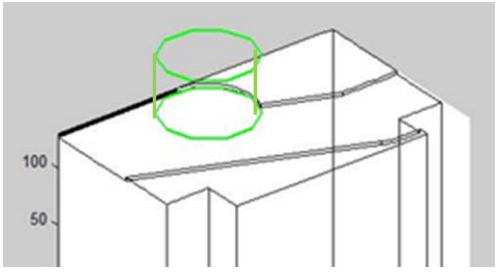

Fig. 9: Cutting test #1, simplified visualization of the tool-workpiece interaction emulated by the geometric engine module

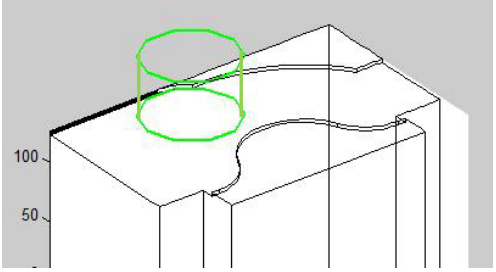

Fig. 10: Cutting test #2, simplified visualization of the tool-workpiece interaction emulated by the geometric engine module

For both of the considered operations, kinematic emulations and geometric simulations (Fig. 9 and Fig. 10) are executed starting from the part programs. The cutting process module provides the estimation of cutting torque and forces, showing the clear effect of the varying engagement conditions (Fig. 11 and Fig. 12). In these cases, the forces are small, in comparison to those related the axis motions (inertia and friction), producing a limited impact on the overall power use. In addition, it has to be noted that the contribution of the axes to the total energy consumption of the drives is very limited and not significant (spindle 98%, axes 2%): this fact can be due to the not relevant masses involved in X and Z axis motion during the tests and to the use of axes rotary motors (efficient from the energy point of view).

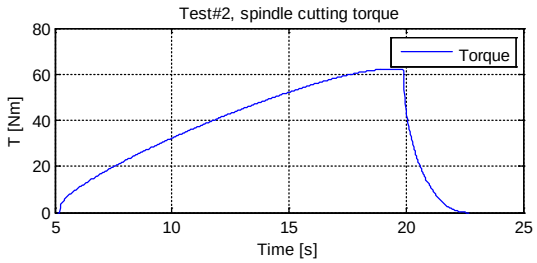

Fig. 11: Test#1, cutting torque during workpiece-tool engagement.

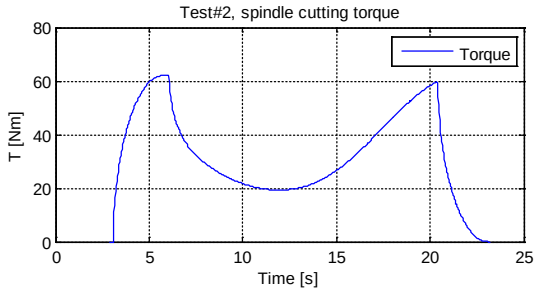

Fig. 12: Test#2, cutting torque during workpiece-tool engagement.

The estimated power consumption provided by the energy evaluator module is compared with the power measured at the spindle drive by a three phases wattmeter inserted between the drive and the motor, sampling the voltages and currents at 200khz (Fig. 13 and Fig. 14). The error between the estimated and measured energy of the spindle is less than 3% for both of the tests (Table 3).

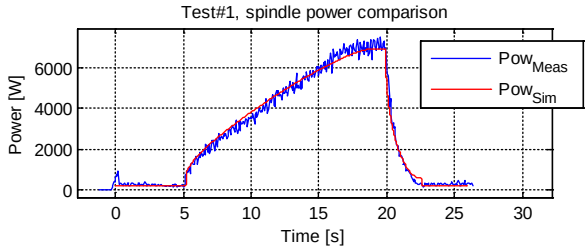

Fig. 13: Test#1, spindle power comparison.

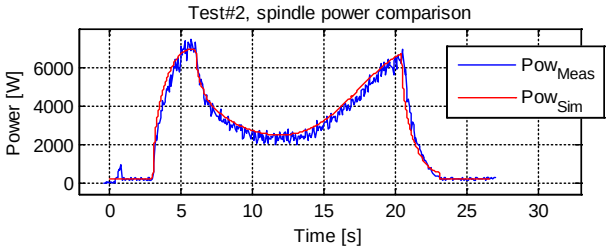

Fig. 14: Test#2, spindle power comparison.

Table 3: Test#1 and Test#2, spindle motor energy consumption comparison

Quantity	Test#1	Test#2
Spindle simulated energy [kJ]	74.261	75.53
Spindle measured energy [kJ]	75.874	75.282
Spindle energy error [%]	-2.13%	0.33%

Considering the measurements, an oscillatory behavior of the spindle motor currents can be noted (see Fig. 15, test#1 taken as example), compared to the smoother simulated one. A time-frequency analysis conducted on the these current signals indicates that the dynamic component is dominated by the tooth passing frequency (in this case occurring at 61.33 [Hz]), phenomenon non represented in the energetic model. In order to verify the possible effect of these oscillations, the dissipated copper losses have been computed (Eq. 1) taking as input respectively the measured spindle quadrature current and same current filtered with a moving average window (Fig. 16). The use of the filter that smooths the oscillation of the measured current bring to an underestimation error of 5% in the estimation of the energy cupper losses. It must be noted that these losses represent a small percentage (8%) of the spindle total energy consumption that is dominated by other contributions, in particular by viscous frictions due to the hydrostatics. These results prove that the choice to not modelling the instantaneous cutting forces does not entail relevant approximations in terms of energy estimation and justify the very low achieved estimation errors, Table 3. So, the performed analysis confirms the initial hypothesis assumed before starting developing the energy-oriented cutting process model.

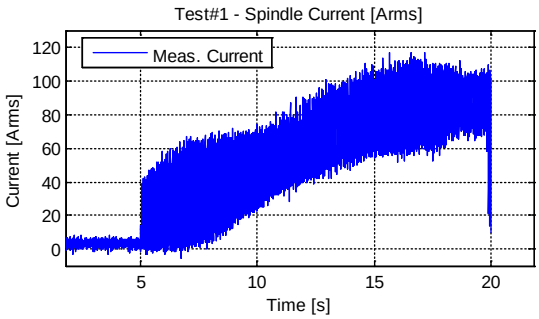

Fig. 15: Test#1, spindle motor measured current.

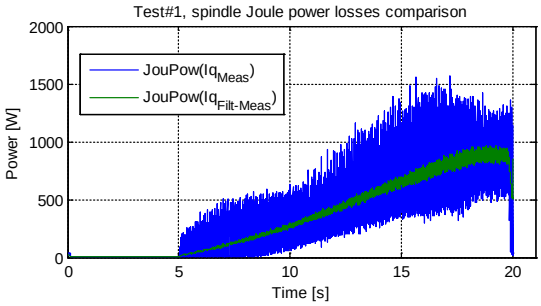

Fig. 16: Test#1, Joule power losses computation using measured current and filtered measured current.

A work cycle for the realization of an open pocket on a C45 steel stock with an end mill (ϕ 37 [mm], 3 inserts). The tool path and the relative part program (two passes with depth of cut of 1.5 [mm], tool path in Fig. 17, part program in Fig. 18) have been generated through the use of a commercial CAM software and have been simulated.

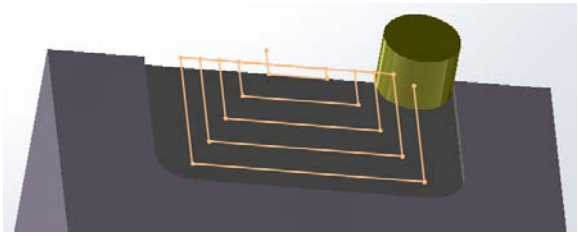

Fig. 17: Open pocket, tool path.

```
N01 G00 X-15. Y160. Z200.
N02 M3 S1720
N03 G00 Y154.
N04 G00 Z178.5
N05 G01 Y130. F516
N06 G01 X15. F516
N07 G01 Y154. F516
N08 G00 X-30.
N09 G01 Y110. F516
N10 G01 X30. F516
N11 G01 Y154. F516
N12 G00 X-40.
N13 G01 Y90. F516
N14 G01 X40. F516
N15 G01 Y154. F516
N16 G00 X-50.
N17 G01 Y70. F516
N18 G01 X50. F516
N19 G01 Y154. F516
N20 G00 X-60.
N21 G01 Y50. F516
N22 G01 X60. F516
N23 G01 Y154. F516
N24 M30
```

Fig. 18: Open pocket, part program.

The spindle motor electrical power consumption estimated by simulation and the one obtained by measurements were compared and a good match can be appreciated (Fig. 19), with a prediction error lower than 5% (Table 4).

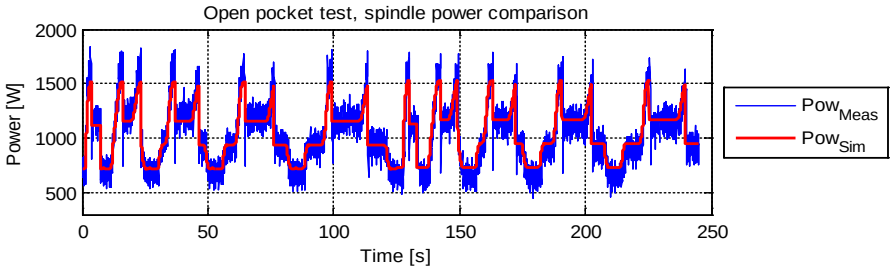

Fig. 19: Open pocket, spindle power comparison.

Table 4: Open pocket, spindle motor energy consumption comparison

Quantity	Open pocket test
Spindle simulated energy [kJ]	245.38
Spindle measured energy [kJ]	254.15
Spindle energy error [%]	-3.45%

5.3 Comparison with energy models from literature

The proposed simulation approach was compared with energy modeling approaches from the literature, in terms of accuracy of energy consumption prediction. Given a literary review, a numerical representation commonly adopted by many authors [9] [11] defines energy consumption of a machine tool as sum of the energy required to start-up and maintain the machine equipment in a "ready" position, and the one required for chip removal, proportional to the quantity of material being processed. This approach, taken as benchmark and indicated in the following with the acronyms "Model-B", is formalized in Eq. 16. Energy is then obtained integrating the power along the time.

$$P = P_0 + P_c = P_0 + k \cdot MRR \qquad \text{Eq. 16}$$

where P is the total power [W], P_0 is the idle power (in this case only the part associated to spindle and axis drives), P_c is the cut-dependent power [W], MRR is the material removal rate [mm^3/s], k is an equivalent cutting process coefficient [J/mm^3]. The idle power represents the constant basal consumption of the machine and its elements, while k comes from the physics of the considered process.

Firstly, the parameters P_0 and k of the already known modelling approach were experimentally characterized from power measurements on Mandelli M5 machine tool application. Focusing the attention only on electro-mechanics of the machine, unknown parameters were estimated by measuring spindle power during execution of milling tests on a C45 steel parallelepiped stock with a face mill tool (ϕ 80 [mm], 4 inserts). The adopted cutting conditions are reported in Table 5.

Table 5: Cutting test conditions for alternative energy model characterization

Parameter	I	II	III	IV	V	VI
Depth of cut [mm]	1.5	2.0	1.5	2.0	1.5	2.0
Width of cut [mm]	30	30	30	30	30	30
Spindle speed [rpm]	1400	1400	800	800	800	1400
Feed per tooth [mm/tooth]	0.10	0.20	0.10	0.20	0.25	0.25
MRR [cm^3/s]	25.2	67.2	14.4	38.4	600	1400
Feed rate [mm/min]	560	1120	320	640	36	84

A least square method is used to estimate the unknown parameters P_0 467.58 [W] and k 2.41 [N/mm^2].

The open pocket test case was used in order to compare the prediction ability of the two approaches. It can be noted that Model-B, that takes as input an average value of material removal rate MRR 11253.6 [mm^3/min] obtained dividing the total removed material volume by the operation time, provides a worse estimation of the spindle energy consumption (Table 6). Model-B does not consider the effect of the velocity on the energy consumption: so, it can be subjected to energy estimation errors, in particular in presence of positioning rapid motions. This is mainly true in case of production of not simple technological features or more complex workcycles.

Table 6: Open pocket, model validation

Quantity	Simulation approach	Model-B
Spindle estimated energy [kJ]	245.38	225.49
Spindle measured energy [kJ]	254.15	254.15
Spindle energy error [%]	-3.45%	-11.30%

5.4 Sensitivity analysis

A sensitivity analysis was performed to evaluate the performance of the developed energy simulator. A first batch of simulations, emulating the cutting test #2 (previously introduced in chapter 5.2) and executed varying the value of tolerance parameter of the geometrical environment, does not provide significant differences between the runs in terms of elaboration time and energy prediction capability. The main affecting parameter on computational time and energy estimation accuracy is the step length used for the tool path discretization. Less is the selected step, greater is the number of points for the computation, obtaining a high precision of the energy consumption calculation in spite of an increase of

the elaboration time. A campaign of simulations based on the emulation of the test #2 was performed and the results are reported in Table 7.

Table 7: Test#2, simulation campaign for sensitivity analysis

	1	2	3	4	5	6	7	8	9	10
Environment geometric tolerance [mm]	10^{-4}	10^{-4}	10^{-4}	10^{-4}	10^{-4}	10^{-4}	10^{-4}	10^{-4}	10^{-4}	10^{-4}
Abscissa step - [%] tool radius	1%	20%	40%	60%	80%	100%	120%	140%	160%	180%
Number of slices	2	2	2	2	2	2	2	2	2	2
Volume of removed material computed in simulation [mm^3]	37772	37709	37518	37122	36664	35988	34881	33053	30394	25664
Elaboration time [s]	89.80	23.73	12.84	10.53	8.73	6.68	6.85	6.32	6.53	4.88
Elaboration / real time ratio [-]	3.22	0.76	0.44	0.34	0.27	0.22	0.26	0.24	0.23	0.17
Estimated Energy [kJ]	75.53	75.39	75.00	74.40	73.88	73.41	71.98	69.17	64.30	56.76
Energy estimation error [%]	0.33%	0.15%	-0.38%	-1.17%	-1.86%	-2.48%	-4.39%	-8.12%	-14.59%	-24.60%

Simulation results (Table 7) confirm that the lack of accuracy in energy estimation in function of the imposed abscissa step distance is due to the error in the calculation of the volume of removed material with small step subtraction logic. In relation to the analyzed test, imposing a step equal to 140% of the tool radius, an acceptable estimation of the energy (<10% respect to the measure) can be obtained in a few seconds of computation. In general, simulation times lower than the time taken to really execute the milling test on the machining center can be obtained adopting a step distance greater than 20% of the tool radius.

The obtained results are summarized in Fig. 20 and Fig. 21.

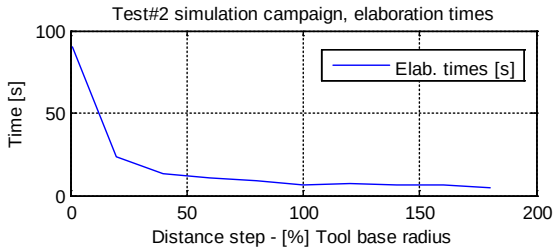

Fig. 20: Test#2 simulation campaign, elaboration times

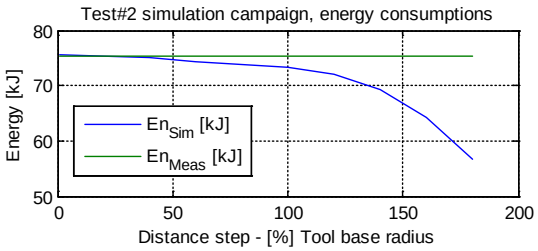

Fig. 21: Test#2 simulation campaign, energy comparison

6 CONCLUSION

In this paper a simulation approach for estimating the energy absorbed by a machine tool during the execution of a generic part program composed of milling operations is proposed. Based on a modular modeling approach, the proposed simulator is able to predict the energy absorbed by the main relevant machine elements. Differently from other literature works, an explicit representation of the cutting process is integrated within the energy modeling of the machine tool. The geometric simulation of the material removal process feeds a detailed mechanistic model for the calculation of the average cutting forces and torque. The computed cutting process-related quantities are used for used energy estimation. In this paper, the focus was put on the estimation capability of the energy taken by the spindle and the machine tool axis. The developed energy models were experimentally characterized and identified by means of a procedure that can be easily used in an industrial scenario. The developed approach was applied to a Mandelli CNC machine. Power measurements performed during experimental milling tests were used to validate the simulator energy estimating

capabilities. The performed milling operations include non-stationary tool-workpiece engagement. Both the absorbed energy prediction accuracy and the simulator computational time were critically analyzed and discussed, comparing to the results achievable adopting other approaches proposed in the literature [9].

Future analyses will be focused on the validation of the proposed simulation approach considering the energy behavior of other machine peripherals, like the hydraulic power and the cutting fluid units. Moreover, the proposed energy simulator could be tested in a more challenging scenario that involves, for instance, a complex machining work-cycle. The information computed during the geometric simulation of the cutting process could be used to calculate other KPIs, in addition to the energy consumption, for instance linked to process dynamics (e.g. stability, vibration) or the tool wear, to support optimizing of additional performances.

7 ACKNOWLEDGEMENTS

The authors would like to thank Dipl-Ing. Mattia Torta for assistance on the measurements. This work has been developed within the activities of the "CTN01_00163_148175 Sustainable Manufacturing" Project.

8 REFERENCES

1. **European Commission.** Eco-Design of Energy Related Products – ERPs. *EU Directive 2009/125/EC.* 2009.

2. **Hauschild, M., Jeswiet, J. e Alting, L.** From Life Cycle Assessment to Sustainable Production: Status and Perspectives. *CIRP Annals - Manufacturing Technology.* 2005. Vol. 54, p. 1-21.

3. **Pusaved, F., Krajnik, P. e Kopac, J.** Transitioning to sustainable production. Part I. Application of machining technologies. *Joutnal of Cleaner Production.* 2010. Vol. 18, 2, p. 174-184.

4. **European Commission.** EuP Eco-Design of Energy using Products. *EU Directive 2005/32/EC.* 2005.

5. **Cecimo.** Concept Description for CECIMO's Self-Regulatory Initiative. *SRI.* 2009. Available at http://www.cecimo.eu/ecodesign-eup/selfregulation.html.

6. **Fraunhofer-IZM.** EC Product Group Study related to the Eco-design of Energy-related Products (ErP). *Directive 2009/125/EC (recast of the former EuP Directive 2005/32/EC) for ENTR Lot 5 Machine Tools.* 2011. Available at http://www.ecomachinetools.eu/typo/ .

7. **ISO.** TC 39 WG 12 (14955) - Envirnmental evaluation of machine tools (metal cutting and metal forming). 2012. Web: http://www.iso.org/iso/iso_technical_committee.html?commid=48354.

8. **Diaz, N., Redelsheimer, E. e Dornfeld, D.** Energy Consumption Characterization and Reduction Strategies for Milling Machine Tool Use. *Proceedings of the 18th CIRP International Conference on Life Cycle Engineering.* Braunschweig, Germany : s.n., 2011. p. 263-267.

9. **Dahmus, J. B. e Gutowski, T. G.** An environmental analysis of machining. *Proceedings of International Mechanical Engineering Congress and RD&D Expo.* Hanaeim, California, USA : s.n., 13-19 November 2004.

10. **Gutowski, T., Dahmus, J. e Thiriez, A.** Electrical Energy Requirements for Manufacturing Processes. *Proceedings of 13 th CIRP International Conference on Life Cycle Engineering.* Lueven, Belgium : s.n., 2006.

11. **Kara, S. e Li, W.** Unit process energy consumption models for material removal processes. *CIRP Annals - Manufacturing Technology.* 2011. Vol. 60, p. 37-40.

12. **Draganescu, F., Gheorghe, M. e Doicin, C. V.** Models of machine tool efficiency and specific consumed energy. *Journal of Materials Processing Technology.* 2003. Vol. 141, 1, p. 9-15.

13. **Mori, M., et al., et al.** A study on energy efficiency improvement for machine tools. *CIRP Annals - Manufacturing Technology.* 2011. Vol. 60, p. 145-148.

14. **Rajemi, M. F., Mativenga, P. T. e Aramcharoen, A.** Sustainable machining: selection of optimum turning conditions based on minimum energy consideration. *Journal of Cleaner Production.* 2010. Vol. 18, 10-11, p. 1059-1065.

15. **Newman, S.T., et al., et al.** Energy efficient process planning for CNC machining. *CIRP Journal of Manufacturing Science and Technology.* 2012. Vol. 5, 2, p. 127-136.

16. **Pavanaskar, S., et al., et al.** Energy-efficient vector field based toolpaths for CNC pocket machining. *Journal of Manufacturing Processes.* 2015. Vol. 20, 1, p. 314-320.

17. **Anderberg, S., Beno, T. e Pejryd, L.** Energy and Cost Efficiency in CNC Machining from a Process Planning Perspective. *9th Global Conference on Sustainable Manufacturing.* St. Petersburg, Russia : s.n., 2011.

18. **Avram, O. I. e Xirouchakis, P.** Evaluating the use phase energy requirements of a machine tool system. *Journal of Cleaner Production.* 2011. Vol. 19, 6-7, p. 699-711.

19. **Abele, E., Eisele, C. e Schrems, S.** Simulation of the Energy Consumption of Machine Tools for a Specific Production Task. *Leveraging Technology for a Sustainable World.* s.l. : Springer, 2012. p. 233-237.

20. **Braun, S. e Heisel, U.** Simulation and Prediction of Process-Oriented Energy Consumption of Machine Tools. *Leveraging Technology for a Sustainable World.* s.l. : Springer, 2012. p. 245-250.

21. **He, Y., et al., et al.** Analysis and estimation of energy consumption for numerical control machine. *Journal of Engineering Manufacturing*. 2012. Vol. 226, B2, p. 255-266.

22. **Borgia, S., et al., et al.** Machine tool energetic simulation during general milling operations. *Proc. of the 3rd International Chemnitz Manufacturing Colloquium on Innovations of Sustainable Production for Green Mobility.* Chemnitz, Germany : s.n., 2014.

23. **Albertelli, P., et al., et al.** Evaluation of the Energy Consumption in Machine Tools: a combined analytical-experimental Approach. *Proceedings of 13th International Conference on The Modern Information Technology in the Innovation Processes on the Industrial Enterprises.* Trondheim, Norway : s.n., 22-24 June 2011.

24. **NUM, Schneider Electric.** SimuCN, version 1.2.18. *Project GIPMO Thème simulation: Simulateur CN*. 2000.

25. **Ehmann, K. ., Kapoor, S. G. e Lazoglu, I.** Machining process modeling: a review. *journal of Manufacturing Science and Engineering.* 1997. Vol. 199, 4-B, p. 655-663.

26. **Altintas, Y.** Manufacturing Automation. s.l. : Cambridge University Press, 2012. ISBN 978-0521172479.

27. **JSA.** TS B 0024-1 Machine Tools - Test Methods for Electric Power Consumption - Part 1: Machining Centres. 2010.